Temperature and wavelength dependence of the thermo-optical properties of tellurite and chalcogenide glasses

K. C. Silva, O. A. Sakai, A. Steimacher, F. Pedrochi, M. L. Baesso, A. C. Bento, A. N. Medina, S. M. Lima, R. C. Oliveira, J. C. S. Moraes, K. Yukimitu, E. B. Araújo, M. Petrovich, and D. W. Hewak

Citation: Journal of Applied Physics **102**, 073507 (2007); doi: 10.1063/1.2786033
View online: http://dx.doi.org/10.1063/1.2786033
View Table of Contents: http://scitation.aip.org/content/aip/journal/jap/102/7?ver=pdfcov
Published by the AIP Publishing

Temperature and wavelength dependence of the thermo-optical properties of tellurite and chalcogenide glasses

K. C. Silva, O. A. Sakai, A. Steimacher, F. Pedrochi, M. L. Baesso, A. C. Bento, and A. N. Medina[a)]
Departamento de Física, Universidade Estadual de Maringá, Av. Colombo 5790, 87020-900, Maringá, Parana, Brazil

S. M. Lima
Grupo de Espectroscopia Óptica e Fototérmica, Universidade Estadual de Mato Grosso do Sul, C.P. 351, Dourados, Mato Grosso do Sul, Brazil

R. C. Oliveira, J. C. S. Moraes, K. Yukimitu, and E. B. Araújo
Grupo de Vidros e Cerâmicas, Universidade Estadual Paulista, C. P. 31, Ilha Solteira, São Paulo, Brazil

M. Petrovich and D. W. Hewak
Optoelectronics Research Center, University of Southampton, Southampton SO17 1BJ, England, United Kingdom

(Received 22 May 2007; accepted 6 August 2007; published online 3 October 2007)

The refractive index and the temperature coefficient of the optical path length change of tellurite ($80TeO_2:20Li_2O$) and chalcogenide glasses ($72.5Ga_2S_3:27.5La_2O_3$) were determined as a function of temperature (up to 150 °C) and wavelength (in the range between 454 and 632.8 nm). The tellurite glass exhibits the usual refractive index dispersion in the wavelength range analyzed, while anomalous refractive index dispersion was observed for the chalcogenide glass between 454 and 530 nm. The dispersion parameters were determined by means of the single-effective oscillator model. In addition, a strong dependence of the temperature coefficient of the optical path length on the photon energy and temperature was found for the chalcogenide glass. The latter was correlated to the shift of the optical band gap (or electronic edge) with temperature, which was interpreted by the electron-phonon interaction model. © *2007 American Institute of Physics*.
[DOI: 10.1063/1.2786033]

I. INTRODUCTION

It is well recognized that the choice of suitable host materials is crucial to the development of novel and more efficient optical devices.[1] Tellurite and chalcogenide glasses are attractive as hosts due to their high refractive index, low phonon energy, and wide transparency window ranging from the visible to the mid-IR.[2,3] The high refractive index correlates with large emission cross sections, and the low phonon energy with reduced nonradiative rates, leading to high quantum efficiencies of radiative transitions. Furthermore, these glasses can accept in their network large amounts of rare earth ions, which opens up the possibility of efficient upconversion lasers.[4] In addition, the high solubility of rare earth makes chalcogenides and tellurites promising candidates for the development of high density optical data storage and displays.[2] The low glass transition temperature of these glasses represents a potential advantage for photonic applications.[5] Chalcogenides, in particular, exhibit amorphous semiconductor behavior, in that they have band gap energies ranging from 1 to 3 eV. They also exhibit strong photorefractive effects, such as photodarkening, reversible photostructural changes, and photoinduced phase changes, which have been explored for the fabrication of photonic integrated circuits.[6,7] In order to make it possible to exploit the potential of these glasses it is paramount to investigate in detail their thermo-optical and other properties; especially their refractive index (n) and the temperature coefficient of optical path length change (dS/dT), which define the propagation characteristics of laser beams within these materials.

In this work we investigated the temperature and wavelength dependences of dS/dT and the wavelength behavior of n in tellurite glasses of molar composition $80TeO_2:20Li_2O$ (TeLi) and oxychalcogenide glasses with molar composition $72.5Ga_2S_3:27.5La_2O_3$ (GLSO). We measured the refractive index, at room temperature, and the temperature coefficient of the optical path length. The refractive index was measured at different wavelengths in the range of 454–530 nm, while dS/dT was measured as a function of both wavelength and temperature. The focus of the discussion will be the evaluation of the behavior of these two quantities in the vicinity of the electronic absorption edge.

II. EXPERIMENTAL

GLSO chalcogenide glass was prepared from Ga_2S_3 and La_2O_3 precursors by standard powder melting.[8] The gallium sulphide was synthesized from electronic-grade gallium metal, achieving a purity, measured by glow discharge mass spectroscopy, of approximately 99.9999%. The lanthanum oxide was commercial purity grade, 99.999%. Batches with

[a)]Author to whom correspondence should be addressed. Electronic mail: medina@dfi.uem.br

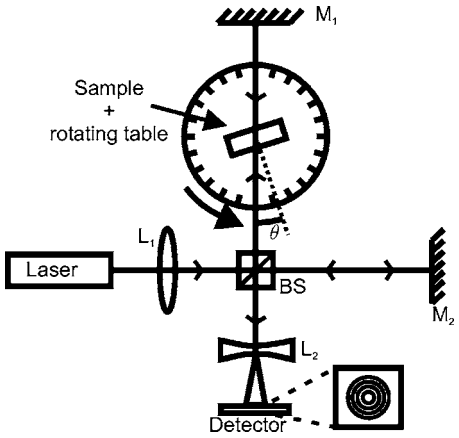

FIG. 1. Experimental setup for refractive index measurements using a modified Michelson-Morley interferometer (L1 and L2: lenses, M1 and M2: mirrors, BS: beam splitter).

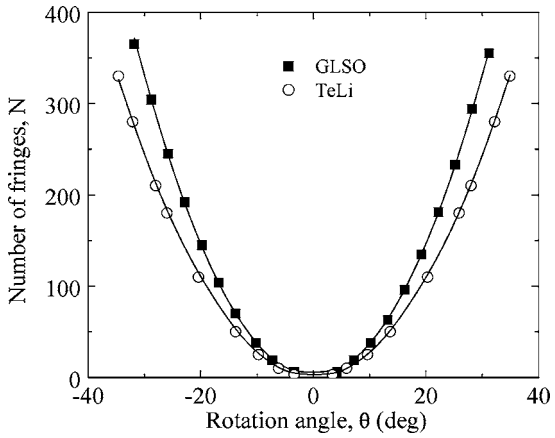

FIG. 2. Number of fringes (N) as function of rotation angle θ measured at $\lambda = 514.5$ nm for GLSO and TeLi glasses. The curves are fits obtained using Eq. (1).

the chosen composition were weighed inside a glovebox, under dry and inert atmosphere, loaded in vitreous carbon crucibles and then transferred to a quartz-lined furnace. Melting was performed at 1150 °C for 24 h under a stream of argon; glass quenching was accomplished by pushing the crucible into a water-cooled jacket.

Tellurite glass had nominal molar composition $20Li_2O$; $80TeO_2$ (TeLi) and was prepared from Li_2CO_3 (Alfa Aesar, 99%) and TeO_2 (Alfa Aesar, 99.95%) using the conventional method.[9] Batches of 15 g were weighed, mixed, and then melted in a platinum crucible at 900 °C for 30 min. The melt was quenched into a mould, obtaining clear, pale yellow ingots, approximately 8 mm thick. Tellurite and chalcogenide glass ingots were annealed, cut in a rectangular shape of approximately 2×1 cm^2 surface area and 1 mm thickness; the flat surfaces were optically polished.

The refractive index n and the optical path length dS/dT were measured using an interferometric techniques. We performed measurements at several wavelengths, using a He–Ne laser at 632.8 nm (Coherent; Model No. 31-2058), a frequency doubled Nd-YAG (YAG denotes yttrium aluminum garnet) laser at 532 nm (Coherent; Model No. BWT-50-E), and a tuneable argon-ion laser with eight lines in the range from 454 to 514.5 nm (Coherent; Model: Innova-90 Plus).

The refractive index measurements were performed using a modified Michelson-Morley interferometer (MMI), as shown in Fig. 1. Here, a rectangular sample with optically polished surfaces is inserted in one arm of the MMI and oriented at an angle θ relative to the laser beam. By varying the angle θ, a shift of the fringe pattern $N(\theta)$ is observed, from which the refractive index of the sample can be determined. The relationship between $N(\theta)$ and θ is given by the following equation:[10,11]

$$N(\theta) = \left(\frac{2L}{\lambda}\right)(1 - n - \cos\theta + \sqrt{n^2 - \sin^2\theta}). \quad (1)$$

In which L is the sample thickness and λ is the laser wavelength.

The interferometric technique used to measure dS/dT is described in detail elsewhere.[12] In the present study, the glass sample was positioned inside an oven, in order to obtain temperature-resolved measurements. The oven temperature was set through a calibrated PT-100 sensor and a temperature controller (Lakeshore Cryonics Inc.—Model No. 340) with a resolution better than 0.01 °C. As the laser beam was passed through the sample, the two parallel surfaces acted like a Fabry-Perot interferometer, producing interference fringes in the reflected intensity. By varying the temperature, the optical path length of the sample changes and a shift in the fringes pattern was observed, which was measured by a photodiode. The signal was fed into a nanovoltmeter (Keithley—Model No. 2182) and stored in a microcomputer. The obtained interference fringe pattern was then used to calculate dS/dT through the following equation:[12]

$$\frac{dS}{dT} = \left(\frac{dn}{dT}\right) + n\alpha = \frac{\lambda}{2L}\left(\frac{dm}{dT}\right). \quad (2)$$

In which, α is the linear thermal expansion coefficient, dn/dT is the refractive index temperature coefficient, and dm/dT is the rate of fringes movement with temperature.

III. RESULTS AND DISCUSSION

Figure 2 shows a typical fringe pattern shift measured as function of the rotation angle for TeLi and GLSO glasses at $\lambda = 514.5$ nm. The curves represent the fits obtained by using Eq. (1), which provides the refractive index for the two glasses ($n = 2.071$ and 2.314 for TeLi and GLSO, respectively). Similar curves were determined for other wavelengths, and the dispersion curves of refractive index are plotted in Fig. 3. The value of refractive index for TeLi glass increases ($\sim 2.5\%$) monotonically with increasing the photon energy. In contrast, the refractive index of GLSO glass shows a maximum at 532 nm and decreases at shorter wavelengths (by approximately 25% at 476 nm). Also shown in Fig. 3 are the absorption spectra of the two glasses at room temperature, measured by using a conventional photoacoustic spectrometer (PAS) (Ref. 13) using frequency modulation of 20 Hz. The spectrum of GLSO clearly shows that the anomalous refractive index dispersion falls in the proximity of the electronic absorption edge. It is also interesting to note that the UV absorption edges are around 410 nm (3.0 eV)

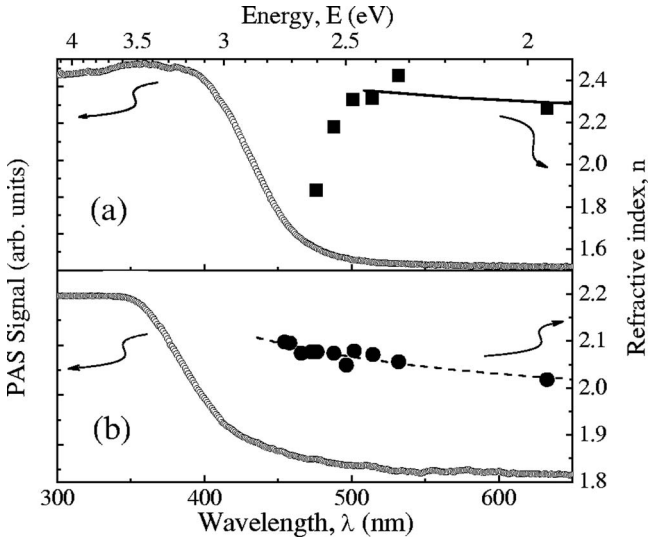

FIG. 3. Room temperature refractive index and absorption as function of wavelength for (a) GLSO and (b) TeLi glasses. Solid line is a simulation using the data of Yayama *et al.* (Ref. 20). The dashed line is a fit using the single-effective oscillator model described in the text. The uncertainty in refractive index is $\pm 2 \times 10^{-3}$.

and 450 nm (2.75 eV) for TeLi and GLSO glasses, respectively. The absorption edge of 410 nm for TeLi glass is consistent with the results found in the literature for other tellurite glasses.[1,14] The GLSO glass presents a blue shift for the absorption edge as compared to a chalcogenide with nominal molar composition 70% Ga_2S_3: 30% La_2S_3 (GLS).[15] This shift has been attributed to the ionic character of the La–O bonds in contrast to the covalent character of Ga–S, which is a dominant factor in the thermo-optics properties of the GLS glass.[16]

The refractive index dispersion of TeLi glass at wavelengths above the optical band gap can be described through the single-effective oscillator model proposed by Wemple[18] and Wemple and DiDomenico,[17]

$$n^2(E) - 1 = \frac{E_d E_0}{(E_0^2 - E^2)}. \tag{3}$$

In which E is the photon energy, E_0 is the energy of the effective dispersion oscillator, and E_d is the dispersion energy. The latter quantity measures the average strength of the interband optical transitions.

By plotting $(n^2-1)^{-1}$ against E^2 it is possible to determine the oscillator parameters. The values of E_0 and E_d can be determined when the refractive index for the wavelength lies far from the electronic edge, using the slope $(E_0E_d)^{-1}$ and the linear (E_0/E_d) coefficients. Under these conditions the refractive index for wavelengths is given by $n_0^2 = 1 + E_d/E_0$. The obtained values for TeLi were $E_d = (19 \pm 1)$ eV, $E_0 = (6.8 \pm 0.7)$ eV, and $n_0 = (1.96 \pm 0.09)$. The dashed line shown in Fig. 3(b) is the best fit calculated using Eq. (3).

The parameter E_d in the Wemple-DiDomenico model is found to obey a simple empirical relationship, i.e., $E_d = \beta N_c Z_a N_e$, in a variety of covalent and ionic crystalline solids. In the latter relationship, N_c is the coordination number of the nearest cation to the anion, Z_a is the formal anion valence, N_e is the effective number of valence electrons of the ion, and β is a constant which is experimentally found to assume essentially two values: $\beta = 0.26$ in ionic materials and $\beta = 0.37$ in covalent materials.[17] Crystalline TeO_2 is a sixfold-coordinated oxide and has $N_c = 6$, $Z_a = 2$, and $N_e = 8$, while crystalline Li_2O has $N_c = 4$, $Z_a = 1$, and $N_e = 8$. For the TeLi glass, we estimated N_c, Z_a, and N_e as the molar average of the values relative to the two glass components. Assuming $\beta = 0.26$, it results in $E_d = 21$ eV, which is in good agreement with the value obtained in this study.

It should be noted that, in amorphous materials, incomplete or dangling bonds and voids generally reduce both the density and the coordination number as compared to the corresponding crystalline phases. These considerations were summarized by Wemple[18] in the following relationship:

$$\frac{E_d^a}{E_d^x} = \frac{\rho^a}{\rho^x} \frac{N_c^a}{N_c^x}. \tag{4}$$

In which ρ indicates the density, and the superscripts a and x refer to the amorphous and crystalline phases, respectively. According to this formula, the smaller dispersion energy E_d in amorphous glasses can be attributed to the lower coordination and density of their network.

As mentioned above, GLSO glass has anomalous refractive index dispersion below 500 nm, which can be interpreted as a consequence of the proximity to the electronic absorption edge.[19] In this wavelength region, the Wemple-DiDomenico model cannot be applied.

However, recently Yayama *et al.*[20] showed that the refractive index dispersion curve could be determined in wavelengths above the band gap (up to 1.71 μm) for GLSO glass with molar concentration 70 Ga_2S_3: 30 La_2O_3. Using the Wemple and DiDomenico relationship, we estimated $E_0 = 6.4$ eV and $E_d = 24.6$ eV for this glass. The solid line in Fig. 3(a) is the simulated curve calculated from Eq. (3) using these values of E_0 and E_d, showing a good agreement with our experimental data for energies about the optical band gap. Therefore, we used theses values and estimated $n_0 = 2.20$ to our GLSO glass sample.

Figure 4 shows the temperature dependence of dS/dT for GLSO (a) and TeLi (b) samples for different wavelengths. The values of dS/dT measured for TeLi glass are generally lower than those of GLSO glass. At 632.8 nm, for instance, dS/dT is nearly three times larger in GLSO. The linear increase of dS/dT with the temperature was observed at all investigated wavelengths. This observation is, for instance, very important for the development of laser devices, in which the active medium can reach temperatures of the order of 150 °C,[21,22] thus causing an increase of dS/dT, and, ultimately, degradation of the beam quality. It should also be noted that the slope exhibits a strong dependence on the photon energy. For instance, the slopes measured at 476.5 nm for TeLi and GLSO are 5.4×10^{-8} and 8.7×10^{-8} K^{-2}, respectively, which are 3.5 and 2.5 times larger than those at 632.8 nm.

It is interesting to point out that dS/dT carries information about the thermal expansion coefficient and changes in the electronic polarizability which are both dependent on the sample temperature.[23–25] Since the thermal expansion coefficient is independent of the wavelength, then the wavelength

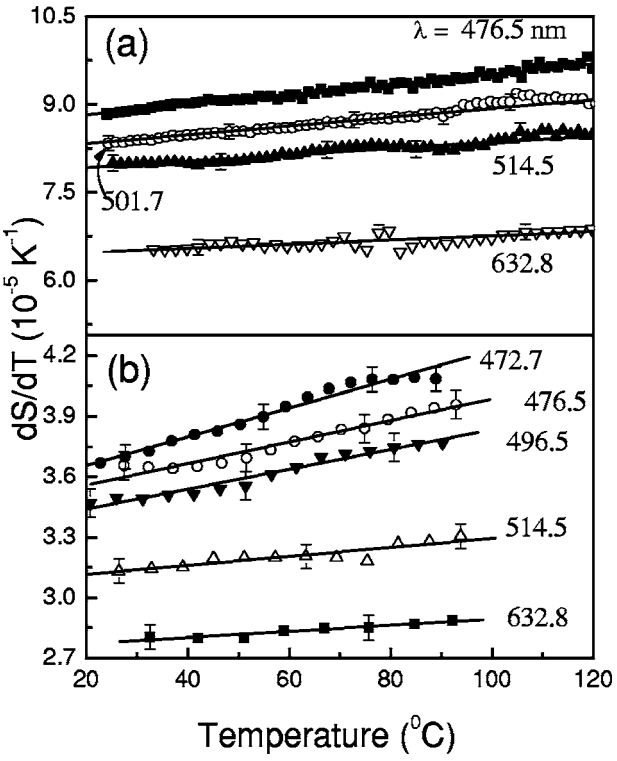

FIG. 4. Temperature coefficient of the optical path length (dS/dT) as function of temperature for GLSO (a) and TeLi (b) glasses at different wavelengths. Lines are linear fits to the data.

dependence of dS/dT at a fixed temperature provides information on the wavelength dependence of the electronic polarizability of the glass. The dispersion curves of dS/dT at 65 °C are shown in Fig. 5(a). An increase of about 50% was observed for both glasses if the results for shorter wavelengths are compared to those at 632.8 nm.

The temperature dependence of $dS/dT(T)$ is consistent with that observed in other glass systems[10] and can be attributed to both the thermal expansion coefficient and the temperature coefficient of the refractive index changes (dn/dT).

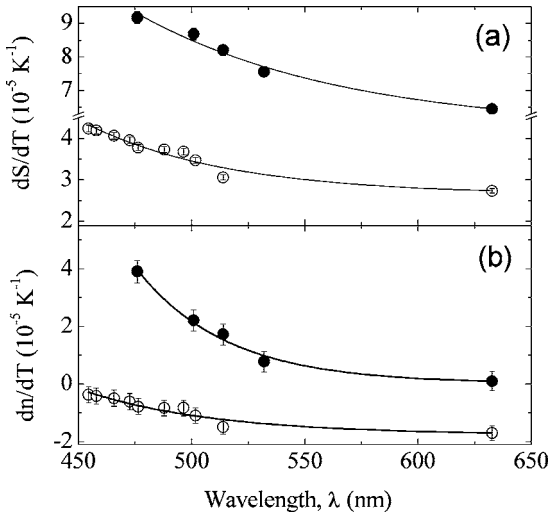

FIG. 5. (a) Temperature coefficient of the optical path length (dS/dT) and (b) temperature coefficient of the refractive index (dn/dT) as function of wavelength for GLSO (full circles) and TeLi (hollow circles) glasses at 65 °C. Lines are shown as a guide to the eye.

On the other hand, the dispersion curves of dS/dT for a fixed temperature [Fig 5(a)] can be used to determine $dn/dT(\lambda)$ through Eq. (2), providing that the coefficient of thermal expansion α is known from complementary measurements. We had recently measured the temperature coefficient of the optical path length change of the glasses analyzed in this study by the thermal lens (TL) method[26,27] [herein denoted as $(ds/dT)_{TL}$]. A value of 4.6×10^{-5} and 1.1×10^{-5} K^{-1} as found at 632.8 nm for GLSO (Ref. 26) and for TeLi,[27] respectively. Note that the quantity $(ds/dT)_{TL}$ is different from that measured in the present study (dS/dT), because in the thermal lens method the sample is excited by a second laser beam inducing a nonhomogeneous heating of the sample. In a TL experiment, the optical path length change is given by[28]

$$\left(\frac{ds}{dT}\right)_{TL} = \frac{dn}{dT} + \alpha(n-1)(1+\nu) + \frac{n^3}{4}Y\alpha(q_{\parallel}+q_{\perp}). \quad (5)$$

In which ν is the Poisson ratio, Y is the Young modulus, and $q_{\parallel}$ and $q_{\perp}$ are the stress-optical coefficient. The second term on the right hand side represents the sample bulging induced by the local heating along the path of the excitation beam. In the case of a thin sample the third term (photoelastic contribution) is very small and can be neglected.[28] By combining Eqs. (2) and (5), it results in

$$\left(\frac{dS}{dT}\right) - \left(\frac{ds}{dT}\right)_{TL} = n\alpha - \alpha(n-1)(1+\nu). \quad (6)$$

The thermal expansion coefficient can thus be determined from the difference between $(ds/dT)_{TL}$ and dS/dT. Using $\nu=0.24$ for GLSO (Ref. 29) and $\nu=0.26$ for TeLi,[30] we obtained $\alpha=(2.8\pm0.2)\times10^{-5}$ K^{-1} and $\alpha=(2.2\pm0.2)\times10^{-5}$ K^{-1} for GLSO and TeLi, respectively. These values are in good agreement with those reported in the literature for other chalcogenide (3.0×10^{-5} K^{-1}) (Refs. 29 and 30) and tellurite (2.2×10^{-5} K^{-1}) (Refs. 31 and 32) glasses. Using these values of α and n in Eq. (2), $dn/dT(\lambda)$ was calculated, and the results are shown in Fig. 5(b).

It is clear from this figure that dn/dT assumes positive values for GLSO and negative for TeLi. This observation can be explained in terms of the model proposed by Prod'homme,[33] who showed that by differentiating the Lorentz-Lorenz relation with respect to the temperature, the following expression for dn/dT can be obtained:

$$\frac{dn}{dT} = \frac{(n^2-1)(n^2+2)}{6n}(\varphi - 3\alpha). \quad (7)$$

In which φ is the thermal electronic polarizability coefficient. The above relationship can account for both positive and negative values of dn/dT observed in different glass systems at temperatures below the glass transition T_G, and also for the large negative dn/dT observed in most of glasses at temperatures above T_G.

Since the thermal expansion coefficient does not depend on the incident photon energy, the dispersion curves $dn/dT(\lambda)$ can be used to determine the thermal electronic polarizability coefficient φ using Eq. (7). Figure 6 shows the wavelength dependence of φ for both GLSO and TeLi glasses.

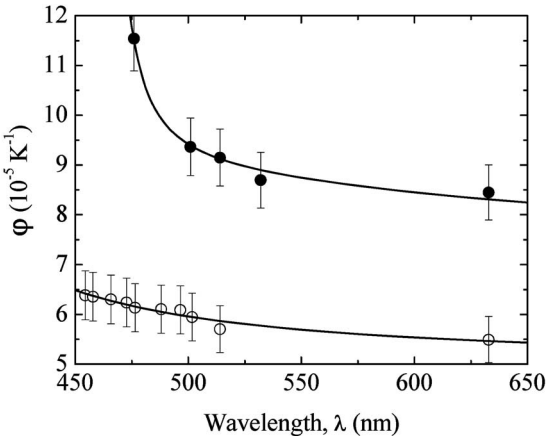

FIG. 6. Thermal electronic polarizability coefficient (φ) as function of wavelength for GLSO (full circles) and TeLi glasses (hollow circles) at 65 °C. Lines are the fits obtained using Eq. (10).

Tsay *et al.*[34] developed an analytical expression for dn/dT in terms of α and the band gap shift with temperature dE_g/dT as

$$2n\frac{dn}{dT} = 4\pi\chi_e\left(-3\alpha - \frac{2}{E_g}\frac{dE_g}{dT}\frac{E_g^2}{E_g^2 - E^2}\right), \tag{8}$$

where χ_e is the electronic susceptibility and E_g is an average value of the optical band gap energy, which we assumed to be defined according to Van Vechten.[35]

By defining $\lambda_g = hc/E_g$ corresponding to the average value of E_g, Eq. (8) can be reformulated in terms of the normalized wavelength $R = \lambda^2/(\lambda^2 - \lambda_g^2)$ as[36,37]

$$\frac{dn}{dT} = \frac{(n_0^2 - 1)}{2n}\left(-3\alpha R - \frac{2}{E_g}\frac{dE_g}{dT}R^2\right). \tag{9}$$

By comparing Eq. (9) with Prod'homme's model [Eq. (7)], the coefficient φ can be expressed as follows:

$$\varphi = 3\alpha + \frac{3(n_0^2 - 1)}{(n^2 - 1)(n^2 + 2)}\left(-3\alpha R - \frac{2}{E_g}\frac{dE_g}{dT}R^2\right). \tag{10}$$

Since n_0, α, and n are known quantities, the values of E_g (or λ_g) and dE_g/dT can be calculated by fitting the φ vs λ curves; we obtained $E_g = (3.7 \pm 0.1)$ eV ($\lambda_g = 336$ nm) and $dE_g/dT = (-1.1 \pm 0.6) \times 10^{-4}$ eV/K for GLSO and $E_g = (4.2 \pm 0.1)$ eV ($\lambda_g = 298$ nm) and $dE_g/dT = (-0.8 \pm 0.3) \times 10^{-4}$ eV/K for TeLi, respectively. These values are in fairly good agreement with the published values for semiconductor materials.[34,37,38]

As expected, the parameter E_g corresponds to an average optical band gap energy and indeed its value is found to be lower in GLSO than in TeLi; for both glasses E_g is about 1.4 times the energy of the electronic absorption edge.

On the other hand, dE_g/dT is approximately 35% larger for GLSO as compared to TeLi glass. This suggests that the position of the electronic edge of GLSO glass is much more dependent on the temperature than in TeLi, and consequently the thermal electronic polarizability coefficient is the dominant term in dn/dT, which consequently causes dn/dT to be positive.

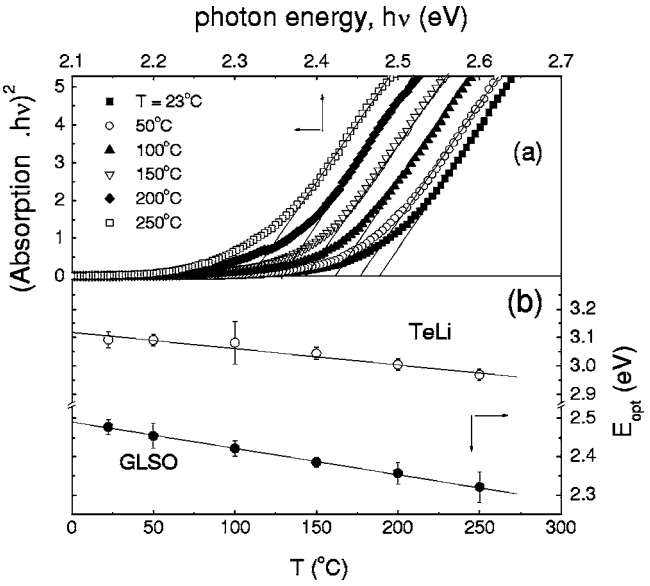

FIG. 7. (a) $(Ah\nu)^2$ as a function of photon energy ($h\nu$) at different temperature of GLSO glass. The lines are fits obtained by using Eq. (11). (b) The electronic absorption edge (E_{opt}) as function of temperature by TeLi and GLSO glasses. Lines are linear fits to the data.

We measured the optical absorption spectra as a function of temperature, and the electronic absorption edge (E_{opt}) was estimated using the model proposed by Tauc *et al.*,[39]

$$(Ah\nu)^m = C(h\nu - E_{opt}) \tag{11}$$

In which, A is the optical absorption, $h\nu$ is the photon energy, C is a constant, and m assumes the values 2 and $\frac{1}{2}$ for direct and indirect gap materials, respectively. For the glasses investigated in this study the best fit was obtained with $m=2$, which correspond to direct gap.[40]

Figure 7(a) shows the square of product $Ah\nu$ as a function of photon energy for GLSO, where the simple lines represent the fit obtained by using Eq. (11), which provides the E_{opt} values. The same procedure was used for TeLi glass (not show here). Figure 7(b) shows the values E_{opt} as a function temperature for both glasses, from which a linear temperature dependence can clearly be inferred. From a linear fit we obtained $dE_{opt}/dT = (-5.8 \pm 0.9) \times 10^{-4}$ eV/K and $dE_{opt}/dT = (-7 \pm 1) \times 10^{-4}$ eV/K for TeLi and GLSO, respectively.

The dE_{opt}/dT values are in fairly good agreement with the published values for semiconductor materials,[34,36,38] and the estimated value for GLSO is larger than those of TeLi glass with expect of dE_g/dT results.

The values of dE_{opt}/dT and dE_g/dT are, however, quite different, which can be explained by considering that E_g is an average value of the optical band gap energy, while E_{opt} is the electronic absorption edge. Despite this difference, the dependence of the optical absorption spectra on the temperature correlates with the dn/dT and dS/dT dispersion curves being dominated by the shift of the electronic absorption band.

It is accepted that two effects are mainly responsible for the temperature dependence of the energy gap, namely, the lattice expansion and the electron-phonon interaction.[38] The latter usually gives the larger contribution; however, a pre-

cise evaluation of its contribution requires a detailed knowledge of the phonon dispersion curves. Several phenomenological models have been proposed to describe the electron-phonon contribution to dE_g/dT. Among these, probably the most accepted are those proposed by Varshni[41] and Pässler.[42] These models predict a linear dependence for the electron-phonon interaction in the limit of high temperature, which is verified by experimental data. Thus, the temperature dependence of E_g, at room temperature, is characterised through dE_g/dT. Consequently, this parameter is of considerable importance particularly with respect to optical integrated devices that are intended to operate within a relatively wide temperature interval, especially at room temperature.

IV. CONCLUSION

In conclusion, in this work the thermo-optical properties of tellurite $(80TeO_2:20Li_2O)$ and oxychalcogenide $(72.5Ga_2S_3:27.5La_2O_3)$ glasses were measured, and their wavelength dispersion and temperature dependence were investigated. Our refractive index results for TeLi suggest that this glass is prevalently ionic, and in fact the coordination number was found to be close to the molar average of coordination of the glass constituents. The temperature coefficient of optical path length change dS/dT was found to increase linearly with increasing the temperature for both glasses, with a rate of increase that is strongly dependent on the wavelength. Combining the results for dS/dT, obtained by interferometric and thermal lens techniques, α and dn/dT were calculated. We found a positive value of dn/dT for GLSO and a negative value for TeLi. This result indicates that the thermal electronic polarizability coefficient is the dominant term in GLSO, while the thermal expansion coefficient is dominant in TeLi glass. The variation of the electronic polarizability coefficient at different wavelengths was attributed to the shift in the band gap energy with temperature; this was used to calculate dE_g/dT. To the best of our knowledge, this is the first time that dE_g/dT has been determined for a tellurite and a chalcogenide glass. Finally, the procedure adopted in the present study could be readily applied to measure the thermo-optical properties of other optical material.

ACKNOWLEDGMENTS

We are thankful to the Brazilian Agencies CNPq, CAPES, and Fundação Araucária for the financial support of this work and to Dr. William Greenhalf for reviewing the manuscript as an English expert.

[1] Y. Gao, Q. H. Nie, T. F. Xu, and X. Shen, Spectrochim. Acta, Part A **61**, 1259 (2005).
[2] P. N. Kumta and S. H. Risbud, J. Mater. Sci. **29**, 1135 (1994).
[3] J. S. Wang, E. M. Vogel, and E. Snitzer, Opt. Mater. (Amsterdam, Neth.) **3**, 187 (1994).
[4] N. K. Giri, A. K. Singh, and S. B. Rai, J. Appl. Phys. **101**, 033102 (2007).
[5] S. Xu, Z. Yang, G. Wang, J. Zang, S. Dai, L. Hu, and Z. Jiang, Spectrochim. Acta, Part A **60**, 3025 (2004).
[6] A. K. Mairaj, P. Hua, H. H. Rutt, and D. W. Hewak, J. Lightwave Technol. **29**, 1578 (2002).
[7] A. V. Kolobov and J. Tominaga, J. Mater. Sci.: Mater. Electron. **14**, 677 (2003).
[8] M. Petrovich, A. K. Mairaj, and D. W. Hewak, *Proceedings of XIX International Congress on Glass*, Edinburgh, Scotland, 2001 (The Society of Glass Technology, Sheffield, UK, 2001), Vol. 2, Extended Abstracts, pp. 951–952.
[9] K. Yukimitu, R. C. Oliveira, E. B. Araújo, J. C. S. Moraes, and L. H. Avanci, Thermochim. Acta **426**, 157 (2005).
[10] K. Betzler, A. Gröne, N. Schimidt, and P. Voigt, Rev. Sci. Instrum. **59**, 652 (1988).
[11] H. El-Kashef, Rev. Sci. Instrum. **65**, 2056 (1994).
[12] A. Steimacher, A. N. Medina, A. C. Bento, J. H. Rohling, M. L. Baesso, V. C. S. Reynoso, S. M. Lima, M. N. Petrovich, and D. W. Hewak, J. Non-Cryst. Solids **348**, 240 (2004).
[13] D. T. Dias, A. N. Medina, M. L. Baesso, A. C. Bento, M. F. Porto, and A. F. Rubira, J. Phys. D **35**, 3240 (2002).
[14] H. Chen, Y. H. Liu, Y. F. Zhou, and Z. H. Jiang, J. Alloys Compd. **397**, 286 (2005).
[15] S. M. Lima, J. A. Sampaio, T. Catunda, A. S. S. de Camargo, L. A. O. Nunes, M. L. Baesso, and D. W. Hewak, J. Non-Cryst. Solids **284**, 274 (2001).
[16] M. N. Petrovich, A. Favre, D. W. Hewak, H. N. Rutt, A. C. Grippo, J. F. Gubeli, K. C. Jordan, G. R. Neil, and M. D. Shinn, J. Non-Cryst. Solids **326**, 93 (2003).
[17] S. H. Wemple and M. DiDomenico, Jr., Phys. Rev. B **3**, 1338 (1971).
[18] S. H. Wemple, Phys. Rev. B **7**, 3767 (1973).
[19] W. K. H. Panofsky and M. Phillips, *Classical Electricity and Magnetism* (Addison-Wesley, Reading, Massachusetts, 1962).
[20] H. Yayama, S. Fujino, K. Morinaga, H. Takebe, D. W. Hewak, and D. N. Payne, J. Non-Cryst. Solids **239**, 187 (1998).
[21] R. Weber, B. Neuenschwander, and H. P. Weber, Opt. Mater. (Amsterdam, Neth.) **11**, 245 (1999).
[22] F. Balembois, F. Druon, F. Falcoz, P. Georges, and A. Brun, Opt. Lett. **22**, 387 (1997).
[23] M. Sparks, J. Appl. Phys. **42**, 5029 (1971).
[24] T. Y. Fan and J. L. Daneu, Appl. Opt. **37**, 1635 (1998).
[25] R. M. Waxler and G. W. Cleek, J. Res. Natl. Bur. Stand., Sect. A **77A**, 755 (1973).
[26] S. M. Lima, A. Steimacher, A. N. Medina, M. L. Baesso, M. N. Petrovich, H. N. Rutt, and D. W. Hewak, J. Non-Cryst. Solids **348**, 108 (2004).
[27] S. M. Lima, W. F. Falco, E. S. Bannwart, L. H. C. Andrade, R. C. de Oliveira, J. C. S. Moraes, K. Yukimitu, E. B. Araújo, E. A. Falcão, A. Steimacher, N. C. G. Astrash, A. C. Bento, A. N. Medina, and M. L. Baesso, J. Non-Cryst. Solids **352**, 3603 (2006).
[28] A. A. Andrade, T. Catunda, I. Bodnar, J. Mura, and M. L. Baesso, Rev. Sci. Instrum. **74**, 877 (2003).
[29] www.chgsouthampton.com/technology/properties/
[30] R. F. Cuevas, L. C. Barbosa, A. N. de Paula, Y. Liu, V. C. S. Reynoso, O. L. Alves, N. Aranha, and C. L. César, J. Non-Cryst. Solids **191**, 107 (1995).
[31] E. M. Marmolejo, E. Granado, O. L. Alves, C. L. César, and L. C. Barbosa, J. Non-Cryst. Solids **247**, 189 (1999).
[32] R. El-Mallawany, Mater. Chem. Phys. **60**, 103 (1999).
[33] L. Prod'homme, Phys. Chem. Glasses **1**, 119 (1960).
[34] Y. Tsay, B. Bendow, and S. S. Mitra, Phys. Rev. B **8**, 2688 (1973).
[35] J. Van Vechten, Phys. Rev. **182**, 891 (1969).
[36] L. K. Samanta, G. C. Ghosh, and G. C. Bhar, Indian J. Phys., B **54B**, 426 (1980).
[37] G. C. Bhar and G. C. Ghosh, Appl. Opt. **19**, 1029 (1980).
[38] P. B. Allen and M. Cardona, Phys. Rev. B **27**, 4760 (1983).
[39] J. Tauc, R. Grigovovici, and A. Vancu, Phys. Status Solidi **15**, 627 (1966).
[40] A. Abu El-Fadl, G. A. Mohamad, A. B. Abd El-Moiz, and M. Rashad, Physica B **366**, 44 (2005).
[41] Y. P. Varshni, Physica (Utrecht) **34**, 149 (1967).
[42] R. Pässler, Phys. Status Solidi B **200**, 155 (1997).